

Bloom-Gilman duality of inelastic structure functions in nucleon and nuclei^a

G. Ricco^(*,**), M. Anghinolfi^(**), M. Ripani^(**),
S. Simula^(***) and M. Taiuti^(**)

(*)Dipartimento di Fisica, Università di Genova
Via Dodecanneso 33, I-16146, Genova, Italy

(**)Istituto Nazionale di Fisica Nucleare, Sezione di Genova
Via Dodecanneso 33, I-16146, Genova, Italy

(***)Istituto Nazionale di Fisica Nucleare, Sezione Sanità
Viale Regina Elena 299, I-00161 Roma, Italy

Abstract

The Bloom-Gilman local duality of the inelastic structure function of the proton, the deuteron and light complex nuclei is investigated using available experimental data in the squared four-momentum transfer range from 0.3 to 5 (GeV/c)². The results of our analysis suggest that the onset of the Bloom-Gilman local duality is anticipated in complex nuclei with respect to the case of the proton and the deuteron. A possible interpretation of this result in terms of a rescaling effect is discussed with particular emphasis to the possibility of reproducing the damping of the nucleon-resonance transitions observed in recent electroproduction data off nuclei.

PACS numbers: 13.60.Hb; 13.60.Rj; 12.40.Nn;14.20.Dh.

^aTo appear in Physical Review C.

1 Introduction.

The investigation of inelastic lepton scattering off nucleon and nuclei can provide relevant information on the concept of parton-hadron duality, which deals with the relation among the physics in the nucleon-resonance and Deep Inelastic Scattering (*DIS*) regions. As is known, well before the advent of *QCD*, parton-hadron local duality was observed empirically by Bloom and Gilman [1] in the structure function $\nu W_2^p(x, Q^2)$ of the proton measured at *SLAC* (where $x \equiv Q^2/2m\nu$ is the Bjorken scaling variable, m the nucleon mass and Q^2 the squared four-momentum transfer). Moreover, it is well established that both the electroexcitation of the most prominent nucleon resonances and the nuclear structure function in the *DIS* region are affected by nuclear medium (cf., e.g., Refs. [2, 3]). In particular, existing data on the electroproduction of nucleon resonances show that the disappearing of the resonance bumps with increasing Q^2 is faster in nuclei than in the nucleon (cf., e.g., Refs. [4], [5] and references therein quoted). Therefore, in this paper we want to address the specific question whether and to what extent the Bloom-Gilman duality already observed in the proton occurs also in the structure function of a nucleus. To this end, all the available experimental data for the structure functions of the proton, the deuteron and light complex nuclei in the Q^2 range from 0.3 to 5 $(GeV/c)^2$ have been analyzed and the Q^2 behaviours of the structure function and its moments are presented for all the targets considered. In case of the proton we observe that the Bloom-Gilman local duality is fulfilled only by the inelastic part of the structure function, while the inclusion of the contribution of the elastic peak leads to remarkable violations of the local duality. In case of complex nuclei, despite the poor statistics of the available data, it is found that the onset of the parton-hadron local duality for the inelastic part of the structure function is anticipated with respect to the case of the proton and the deuteron. Nevertheless, new high-precision nuclear data are needed and, in this respect, it should be mentioned that the Thomas Jefferson National Accelerator Facility (*TJNAF*) is expected to provide in the next future systematic measurements with unprecedented accuracy of the nucleon and nuclear inelastic response to electron probes in the region of nucleon-resonance production for values of Q^2 up to several $(GeV/c)^2$. Finally, a possible interpretation of the observed nuclear modification of the onset of the Bloom-Gilman local duality in terms of a Q^2 -rescaling effect is discussed with particular emphasis to the possibility of reproducing the damping of the nucleon-resonance transitions observed in recent electroproduction data off nuclei [5].

2 The *dual* structure function.

The Bloom-Gilman local duality [1] states that the smooth scaling curve measured in the *DIS* region at high Q^2 represents an average over the resonance bumps seen in the same x region at low Q^2 . More precisely, Bloom and Gilman pointed out the occurrence of a precocious scaling of the average of the inclusive $\nu W_2^p(x', Q^2)$ data in the resonance region to the *DIS* structure function $F_2^p(x')$, at corresponding values of an improved empirical variable $x' = x/(1 + m^2x/Q^2)$. Later on, within *QCD*, a justification of the Bloom-Gilman duality was offered by De Rujula, Georgi and Politzer [6] in terms of the moments $M_n(Q^2)$

of the nucleon structure function $F_2(\xi, Q^2)$:

$$M_n(Q^2) \equiv \int_0^1 d\xi \xi^{n-2} F_2(\xi, Q^2) \quad (1)$$

where ξ is the Nachtmann variable (cf. [7])

$$\xi = \frac{2x}{1 + \sqrt{1 + \frac{4m^2 x^2}{Q^2}}} \quad (2)$$

Using the Operator Product Expansion (*OPE*) the authors of Ref. [6] argued that

$$M_n(Q^2) = A_n(Q^2) + \sum_{k=1}^{\infty} \left(n \frac{\gamma^2}{Q^2} \right)^k B_{nk}(Q^2) \quad (3)$$

where γ^2 is a scale constant. The first term $A_n(Q^2)$ in Eq. (3) is the result of perturbative *QCD*, while the remaining terms $B_{nk}(Q^2)$ are higher twists related to parton-parton correlations. The value of γ^2 is relatively small (a recent estimate, made in Ref. [8], yields $\gamma^2 \sim 0.1 \div 0.3 \text{ GeV}^2$). Therefore, at $Q^2 \gtrsim m^2$ the asymptotic moments $A_n(Q^2)$ are still leading, while resonances contribute to the higher twists $B_{nk}(Q^2)$. The quantities $A_n(Q^2)$ can be considered as the moments of a smooth structure function, which can be identified with the average function $\langle \nu W_2(x, Q^2) \rangle$ occurring in the Bloom-Gilman local duality, namely [7]:

$$\begin{aligned} \langle \nu W_2(x, Q^2) \rangle &= \frac{x^2}{(1 + \frac{4m^2 x^2}{Q^2})^{3/2}} \frac{F_2^S(\xi, Q^2)}{\xi^2} \\ &+ 6 \frac{m^2}{Q^2} \frac{x^3}{(1 + \frac{4m^2 x^2}{Q^2})^2} \int_{\xi}^1 d\xi' \frac{F_2^S(\xi', Q^2)}{\xi'^2} \\ &+ 12 \frac{m^4}{Q^4} \frac{x^4}{(1 + \frac{4m^2 x^2}{Q^2})^{5/2}} \int_{\xi}^1 d\xi' \int_{\xi'}^1 d\xi'' \frac{F_2^S(\xi'', Q^2)}{\xi''^2} \end{aligned} \quad (4)$$

where the ξ -dependence as well as the various integrals appearing in the r.h.s. account for target mass effects in the *OPE* of the hadronic tensor. According to Ref. [7] these effects have to be included in order to cover the low Q^2 region. In Eq. (4) $F_2^S(x, Q^2)$ represents the asymptotic nucleon structure function, fitted to high Q^2 proton and deuteron data [9] and extrapolated down to low values of Q^2 by the Altarelli-Parisi evolution equations [10]. In this paper the Gluck-Reya-Vogt (*GRV*) fit [11], which assumes a renormalization scale as low as $0.4 \text{ (GeV}/c)^2$, will be used to obtain the parton densities $\rho_f(x, Q^2)$ evolved at Next to Leading Order (*NLO*) from sufficiently low Q^2 to cover the range of interest in the present analysis. In the *DIS* region [12] one gets $F_2^S(x, Q^2) = \sum_f e_f^2 x [\rho_f(x, Q^2) + \bar{\rho}_f(x, Q^2)]$.

In what follows, we will refer to the mass-corrected, *NLO* evolved function (4) as the *dual* structure function of the nucleon. We stress that by definition the *dual* function does not contain any higher twists generated by parton-parton correlations, i.e. the twists related to the moments $B_{nk}(Q^2)$ in Eq. (3). It should be mentioned that Eq. (4) suffers from a

well known [13, 14] mismatch; indeed, since $\xi(x=1) = 2/(1 + \sqrt{1 + 4m^2/Q^2}) < 1$, the r.h.s. of Eq. (4) remains positive, while its l.h.s. vanishes, as x approaches the elastic end-point $x = 1$. An alternative approach [13], limited at the twist-4 order, is well behaved at the kinematical $x = 1$ threshold, but it cannot be extrapolated to low values of Q^2 , because an expansion over the quantity m^2x^2/Q^2 is involved. Moreover, inelastic threshold effects, due to finite pion mass, are accounted for neither in the Q^2 evolution nor in the target mass corrections, because they are basically higher-twist effects; then, in order to make a detailed comparison with experimental data in the low Q^2 region, we set the *dual* structure function (4) to zero at $x \geq x_{th}$, where

$$x_{th} = \frac{1}{1 + \frac{m_\pi^2 + 2m_\pi m}{Q^2}} \quad (5)$$

with m_π being the pion mass. Therefore, the investigation of parton-hadron local duality will be limited to values of x not larger than x_{th} (5) and to a Q^2 range between a minimum value Q_{min}^2 , which is of the order of the mass scale μ^2 where the moments of the structure functions $M_n(Q^2)$ start to evolve according to twist-2 operators, and a maximum value Q_{max}^2 ($\gtrsim 5 (GeV/c)^2$ [8]), where the resonance contribution to the lowest moments of Eq. (3) is of the same order of magnitude of the experimental errors.

3 Inclusive data analysis.

The pseudo-data for the proton structure function νW_2^p , obtained from a fit of *SLAC* data at medium and large x [15] and from a fit of the *NMC* data [9] in the *DIS* region, are reported in Fig. 1 versus the Nachtmann variable ξ (2) and compared with the *dual* structure function (4) at fixed values of Q^2 in the range 0.5 to 2 $(GeV/c)^2$. As already pointed out in [6], the onset of local duality occurs at $Q^2 \simeq Q_0^2 \sim 1 \div 2 (GeV/c)^2$.

In case of the deuteron the average nucleon structure function $\nu \bar{W}_2^N \equiv (\nu W_2^p + \nu W_2^n)/2$, obtained from (4), should be folded with the momentum distribution which accounts for the internal motion of the nucleon in the deuteron. The most evident effect of this folding is a broadening of the nucleon elastic peak occurring at $x = 1$ into a wider quasi-elastic peak, partially overlapping the inelastic cross section at large x . In the deuteron the nucleon momentum distribution is relatively narrow and this fact limits the overlap to the kinematical regions corresponding to $x \gtrsim 0.8$. Therefore, it is still possible to subtract the quasi-elastic contribution directly from the total cross section [15]. The folding of the *dual* structure function of the nucleon (Eq. (4)) with the nucleon momentum distribution in the deuteron is performed following the procedure of Ref. [16], which can be applied both at low and high values of Q^2 , at variance with the standard high- Q^2 folding of Ref. [17]. Adopting the deuteron wave function corresponding to the Paris nucleon-nucleon potential [18], our results for the *dual* structure function folded in the deuteron are reported in Fig. 2 at fixed values of Q^2 in the range from 0.5 to 2 $(GeV/c)^2$, and compared with the deuteron structure function per nucleon, $F_2^D(\xi, Q^2) \equiv \nu \bar{W}_2^D(\xi, Q^2)/2$, obtained from the *NMC* data [19] at low ξ and the fits of inclusive data given in Refs. [9] and [15]. Despite the smoothing of nucleon

resonances caused by the Fermi motion, parton-hadron local duality appears to start again at $Q^2 \simeq Q_0^2 \sim 1 \div 2 (GeV/c)^2$.

In case of complex nuclei the analysis of existing inclusive data is complicated by different reasons:

- inclusive data, coming mainly from old experiments generally with poor statistics, is still very fragmented;
- the longitudinal to transverse separation has been done only in case of few measurements carried out in the nucleon-resonance region. An experiment performed at $Q^2 = 0.1 (GeV/c)^2$ [20] in ^{12}C and ^{56}Fe claims a longitudinal to transverse ratio compatible with zero inside experimental errors ($\sim 10\%$), while at $Q^2 \gtrsim 1 (GeV/c)^2$ deep inelastic scattering data are consistent with larger, fairly x independent σ_L/σ_T ratios [21]. However, the sensitivity of the extraction of the nuclear structure function νW_2^A from the total cross section to the longitudinal to transverse ratio turns out to be rather small (not larger than few % when σ_L/σ_T is moved from zero to 20% in the worst kinematical conditions). Therefore, we have simply interpolated all the existing data for σ_L/σ_T in proton and nuclei, averaged on x , as a function of Q^2 only, obtaining the following empirical ratio:

$$\sigma_L/\sigma_T = a \cdot Q^2 \left[e^{-bQ^2} + c \cdot e^{-dQ^2} \right]$$

with $a = 0.014$, $b = 0.07$, $c = 40.8$ and $d = 0.78$. Since the observed dependence of the inclusive nuclear data on the mass number A is weak [22], the nuclear structure function νW_2^A has been determined as a function of ξ for fixed Q^2 bins using data for 9Be [22, 23], ^{12}C [15, 19, 24] and ^{16}O [5]. Therefore, our result could be considered representative of a complex nucleus with $A \simeq 12$;

- since the nucleon momentum distribution is wider in complex nuclei than in the deuteron (cf. [25] and references therein quoted), the quasi-elastic contribution strongly overlaps the inelastic cross section at low values of Q^2 ; moreover, the quasi-elastic peak is known to be affected by final state interaction effects at $Q^2 \lesssim 0.5 (GeV/c)^2$ (cf. [5]). Then, the subtraction of the quasi-elastic contribution is more critical in nuclei;
- nucleon binding can affect nuclear structure function and should be properly taken into account [3];

The calculation of the quasi-elastic contribution has been performed following the approach of Ref. [25], which has been positively checked against *SLAC* data at values of Q^2 of few $(GeV/c)^2$ [25] as well as against jet-target data at lower Q^2 (down to $0.1 (GeV/c)^2$ [5]). An example of the quality of the agreement among the parameter-free predictions of the quasi-elastic contribution to the inclusive $^{12}C(e, e')X$ cross section and available data at the quasi-elastic peak and in its low-energy side for a Q^2 range from 0.5 to 1 $(GeV/c)^2$, is shown in Fig. 3. Furthermore, the *dual* structure function of the nucleon (4) has been folded using again the procedure of Ref. [16], which, in case of complex nuclei, involves the nucleon

spectral function of Ref. [25]; in this way binding effects are taken into account for states both below and above the Fermi level.

After quasi-elastic subtraction, the results obtained for the inelastic nuclear structure function per nucleon, $F_2^A(\xi, Q^2) \equiv \nu W_2^A(\xi, Q^2)/A$, are shown in Fig. 4 for various Q^2 bins, namely: $Q^2 = 0.375 \pm 0.03$; 0.50 ± 0.05 ; 0.75 ± 0.05 ; 1.1 ± 0.2 ; 1.8 ± 0.2 and 4.5 ± 0.5 (GeV/c)². In comparison with the proton and deuteron cases, the most striking feature of our result for nuclei with $A \simeq 12$ is a more rapid smoothing of the resonance bumps with increasing Q^2 , which favours a faster convergence towards the *dual* structure function in the nucleus. This effect, already noticed in Ref. [5] in the Q^2 range from 0.1 to 0.5 (GeV/c)², cannot be completely explained as a broadening of the resonance width due to final state interactions, but some extra-damping factor is needed in order to reproduce the missing resonance strength^b. From Fig. 4 it can clearly be seen that the *dual* structure function (4), properly folded [16] using the nucleon spectral function of Ref. [25], approaches the inelastic data at $Q^2 \simeq Q_0^2 \sim 0.5 \div 1.1$ (GeV/c)², i.e. for values of Q_0^2 lower than those found in the proton and in the deuteron ($Q_0^2 \sim 1 \div 2$ (GeV/c)²).

4 Results and discussion.

All the data obtained for the structure function $F_2^p(\xi, Q^2)$ in the proton, $F_2^D(\xi, Q^2)$ in the deuteron and $F_2^A(\xi, Q^2)$ in nuclei with $A \simeq 12$ (see Figs. 1, 2 and 4) show a systematic approach to the properly folded dual structure function for $\xi \gtrsim 0.2$, the convergence being even more evident and faster in nuclei, due to the fading of resonances already at $Q^2 \gtrsim 0.5$ (GeV/c)².

At smaller values of ξ and for $Q^2 < 5$ (GeV/c)² proton and deuteron data seems to be compatible with an evolution of sea partons slower than the *GRV* prediction; in complex nuclei the difference is further enhanced by the shadowing effect [3]. The reason of this discrepancy is not evident and various motivations can be invoked, like: a breakdown of duality and/or (unexpected) higher twists at low x , or, more likely, a not yet completely consistent initial ($Q^2 \simeq 0.4$ (GeV/c)²) parton density parametrization in *GRV* fit [11].

The minimum momentum transfer Q_0^2 , where local duality provides an acceptable fit to the average inclusive inelastic cross sections, should be related to the mass scale μ^2 , which is defined as the minimum value of Q^2 where the moments of the structure functions $M_n(Q^2)$ begin to evolve according to twist-2 operators, i.e. when $M_n(Q^2) \sim A_n(Q^2)$. Thus, the Q^2 -dependence of all the moments should exhibit a systematic change of the slope at $Q^2 \simeq Q_0^2 \simeq \mu^2$ and then should follow the perturbative *QCD* evolution. The *experimental* $M_2(Q^2)$, $M_4(Q^2)$, and $M_6(Q^2)$ moments have been computed for the proton, the deuteron and nuclei with $A \simeq 12$ according to Eq. (1) using the experimental data for the structure function $F_2^p(\xi, Q^2)$, $F_2^D(\xi, Q^2)$ and $F_2^A(\xi, Q^2)$ shown in Figs. 1, 2 and 4. The results are plotted in Fig. 5 for Q^2 between 0.3 and 5 (GeV/c)². The expected systematic change of the slope is clearly exhibited by all the moments considered and the corresponding values of

^bMedium effects were noticed also in Ref. [26] in the form of a better y -scaling of the inclusive cross section in the region of $P_{33}(1232)$ resonance electroproduction in nuclei with respect to the free nucleon case.

$Q^2 = Q_0^2$ are reported in Table 1. Moreover, in Fig. 6 the relative deviation

$$\frac{\Delta M_n}{A_n}(Q^2) \equiv \frac{M_n(Q^2) - A_n(Q^2)}{A_n(Q^2)} \quad (6)$$

is plotted as a function of Q^2 , where $A_n(Q^2)$ has been computed from the properly folded *dual* structure function (continuous lines in Figs. 1, 2 and 4). Despite the large errors affecting the available nuclear data, in case of all the targets considered the results for $\Delta M_2/A_2$ show a rapid convergence toward A_2 for values of Q^2 very close to the Q_0^2 values of Table 1. For higher moments, the convergence toward A_n is still evident, but it is slower probably because of the presence of resonances at large ξ .

The results presented in Figs. 5 and 6 correspond only to the contribution of the inelastic part of the structure functions to the moments (1). Since in Eq. (1) the integration is extended up to $\xi = 1$, the question of the role played by the contribution of the elastic peak in the nucleon and the quasi-elastic peak in nuclei naturally arises. Therefore, in case of the proton we have considered the contribution $M_n^{(el)}(Q^2)$ resulting from the elastic peak, which reads as

$$M_n^{(el)}(Q^2) = \frac{G_E^2(Q^2) + \tau G_M^2(Q^2)}{1 + \tau} \frac{\xi_p^n}{2 - \xi_p} \quad (7)$$

where G_E (G_M) is the charge (magnetic) Sachs form factor of the proton, $\xi_p \equiv \xi(x = 1) = 2/(1 + \sqrt{1 + 1/\tau})$ and $\tau = Q^2/4m^2$. In Fig. 7 we have reported the results obtained for $M_n^{(tot)}(Q^2) \equiv M_n^{(el)}(Q^2) + M_n(Q^2)$ and $\Delta M_n^{(tot)}(Q^2)/A_n(Q^2)^c$. It can clearly be seen that the higher-twists introduced by the proton elastic peak do not change significantly (within few %) the lowest-order moment $M_2(Q^2)$ for $Q^2 \gtrsim 1.5$ (GeV/c)², whereas they sharply affect higher moments up to quite large values of Q^2 (cf. also Ref. [8]). This means that parton-hadron duality still holds for the total area $M_2^{(tot)}(Q^2)$, i.e. for the average of the structure function over all possible final states, with a mass scale consistent with the one obtained including the inelastic channels only. On the contrary, at least for Q^2 up to several (GeV/c)² the local duality is violated by the elastic peak. This result is consistent with those of Refs. [1, 6], where the applicability of the concept of parton-hadron local duality in the region around the nucleon elastic peak was found to be critical. We have obtained similar results in case of the deuteron, while the analysis of the available nuclear data appears to be compatible within large errors. To sum up, the twist-2 moments $A_n(Q^2)$ dominate the total moments $M_n^{(tot)}(Q^2)$ starting from values of Q^2 which strongly depend upon the order of the moment (see Fig. 7). On the contrary, the Q^2 behaviour of the inelastic contribution $M_n(Q^2)$ is governed by $A_n(Q^2)$ starting from a value $Q^2 \simeq Q_0^2$ almost independent of the order of the moment (see Figs. 5 and 6); thus, after Mellin transformation, the twist-2 operators dominate the inelastic part of the structure function for $Q^2 \gtrsim Q_0^2$ and, therefore, the parton-hadron local duality holds for the averages of the structure function over the nucleon-resonance bumps.

^cWe point out that Eq. (3) holds only for $M_n^{(tot)}(Q^2)$ (cf. Ref. [8]). The elastic contribution (7) *must* be included in Eq. (1) when the extraction of the higher-twists from the moments is required, which is not the case of the present work.

Both the comparison of the moments and the discussion on the onset of the local duality strongly suggest the occurrence of the dominance of twist-2 operators in the inelastic structure functions for values of Q^2 above the Q_0^2 values of Table 1. Therefore, we may argue that present experimental data are compatible with a mass scale $\mu^2 \simeq Q_0^2$; from Table 1 this means: $\mu_N^2 \simeq \mu_D^2 = 1.5 \pm 0.1 (GeV/c)^2$ for the nucleon and the deuteron, and $\mu_A^2 = 1.0 \pm 0.2 (GeV/c)^2$ for nuclei with $A \simeq 12$.

A change of the mass scale of the twist-2 matrix elements in nuclei ($\mu_A^2 < \mu_D^2 \simeq \mu_N^2$) is expected to lead to a rescaling relation for the (inelastic) moments [27, 28], viz.

$$M_n^A(Q^2) = M_n^D(\delta_n(Q^2) \cdot Q^2) \quad (8)$$

with $\delta_n(Q^2 \simeq \mu^2) \simeq \mu_D^2/\mu_A^2$. Assuming a rescaling factor $\delta_n(\mu^2) \simeq \delta$ independent of the order of the moment, the rescaling relation (8) with $\delta = 1.17 \pm 0.09$ brings all the moments in the deuteron and in nuclei into the best simultaneous agreement around the mass scale region, as it is shown in Fig. 8. A possible mechanism for the Q^2 -rescaling has been suggested in Ref. [27]: the quark confinement scale may increase in going from a free nucleon to a nucleus, due to the partial overlap of nucleons in the nuclear medium. The change in the quark confinement size leads to a change in the mass scale μ^2 and one gets $\delta = \mu_D^2/\mu_A^2 = \lambda_A^2/\lambda_D^2$, where λ_D ($\simeq \lambda_N$) and λ_A are the average quark confinement size in the deuteron (nucleon) and in the nucleus, respectively. We stress that the partial quark deconfinement is not the only mechanism yielding a rescaling effect; in this respect, we mention also the model of Ref. [28], where the rescaling mechanism is driven by the off-mass-shellness of the nucleon in the nucleus.

If $\delta_n(Q^2)$ is independent of the order of the moment, then after Mellin transformation the Q^2 -rescaling can be applied to the nuclear structure function per nucleon $F_2^A(x, Q^2)$, viz.

$$F_2^A(x, Q^2) = F_2^D(x, \delta(Q^2) \cdot Q^2) \quad (9)$$

where the virtual photon mass dependence of $\delta(Q^2)$ follows from perturbative QCD evolution at NLO (see [27, 28]). In Fig. 9 existing data on $F_2^A(x, Q^2)$ for nuclei with $A \simeq 12$ are plotted for fixed values of x in a wide Q^2 range. The *dual* structure function (4), properly folded [16] for taking into account nuclear binding effects, is also shown in Fig. 9 for different values of the mass scale ratio μ_D/μ_A . It can be seen that at high Q^2 a mass scale ratio $\mu_D/\mu_A = 1.1$ removes most of the disagreement at large x , but at the price of spoiling the agreement at intermediate values of x . Moreover, at low values of Q^2 the present accuracy of the data does not allow any serious discrimination between different quark confinement ratios. We mention that in Ref. [29] a nucleon swelling corresponding to $\mu_D/\mu_A \simeq 1.075$ has been derived from a combined analysis of the *EMC* effect at small and large x , performed within a constituent-quark picture of the nucleon structure function in nuclei.

To sum up, roughly consistent values of the mass scale ratio μ_D/μ_A between the deuteron and nuclei with $A \simeq 12$ can be obtained in different ways, viz.

- from the onset of local duality (see Table 1 and Fig. 5): $\mu_D/\mu_A = 1.2 \pm 0.1$;

- from the rescaling of the moments at the static point $Q^2 \simeq \mu^2$ (see Fig. 8): $\mu_D/\mu_A = 1.08 \pm 0.05$;
- from the *EMC* effect (see Fig. 9): $\mu_D/\mu_A \lesssim 1.10$.

Nucleon resonances contribute mostly to $M_4(Q^2)$ and $M_6(Q^2)$ (see Fig. 6): the good overlap of these moments in the deuteron and nuclei, observed in Fig. 8 after Q^2 -rescaling, could suggest that a change of the mass scale in nuclei might be consistent with the more rapid decrease of the inelastic $P_{33}(1232)$ and $D_{13}(1520)$ resonance form factors claimed in Ref. [5], where values of Q^2 as low as $0.1 (GeV/c)^2$ are however involved. The *experimental* suppression factor $R_s(Q^2)$, as determined in Ref. [5] using inclusive ^{12}C and ^{16}O data, is reported in Fig. 10 as a function of Q^2 in the region of the $P_{33}(1232)$ resonance production. Assuming that a constant Q^2 -rescaling $\delta(Q^2) \simeq \mu_D^2/\mu_A^2$ can be used below the static point ($Q^2 < \mu^2$), the suppression factor is expected to be given by

$$R_s(Q^2) = \left\{ \frac{G_M^{(N-\Delta)}\left[\frac{\mu_D^2}{\mu_A^2} Q^2\right]}{G_M^{(N-\Delta)}(Q^2)} \right\}^2 \quad (10)$$

where $G_M^{(N-\Delta)}(Q^2)$ is the magnetic form factor of the $N - \Delta$ transition. Using a standard dipole form (for sake of simplicity) and the value $\mu_D/\mu_A = 1.08$, one gets the solid lines shown in Fig. 10 at $Q^2 \lesssim 0.5 (GeV/c)^2$. It can be seen that (surprisingly) a simple Q^2 -rescaling of the dipole ansatz is consistent with the quenching observed for the Δ -resonance electroproduction both in case of the excitation strength alone (see Fig. 10(a)) and for the total inclusive cross section (see Fig. 10(b) and cf. Ref. [31]).

A Q^2 -rescaling effect could in principle be applied also to the elastic form factors of a nucleon bound in a nucleus and it can be viewed as a change of the nucleon radius in the nuclear medium. In this respect, it should be pointed out that: i) in Ref. [32] an increase not larger than $\simeq 6\%$ of the proton charge radius was found to be compatible with y -scaling in 3He and ^{56}Fe ; ii) the analysis of the Coulomb Sum Rule (*CSR*) made in Ref. [33] suggested an upper limit of $\simeq 10\%$ to the variation of the proton charge radius in ^{56}Fe ; iii) recently [34] the experimental value (S_L) of the *CSR* in ^{12}C and ^{56}Fe has been accurately analyzed at $Q^2 \simeq 0.3 (GeV/c)^2$, obtaining a saturation value $S_L = 0.94 \pm 0.13$ and $S_L = 0.97 \pm 0.12$, respectively. If at the same value of Q^2 we would assume the same change of the mass scale ($\mu_D^2/\mu_A^2 \simeq 1.15$) observed in the inelastic channels, an increase of $\simeq 8\%$ for the proton charge radius and a quenching of $\simeq 0.84$ for S_L would be obtained, both being at limit with the quoted errors. However, based on the results shown in Figs. 5-7, it is unlikely that a common Q^2 -rescaling effect could be applied both to the nucleon elastic peak and to the nucleon-resonance transitions.

Before closing, let us make a brief comment on the photoproduction of nucleon resonances. Real photon experiments [35] show that in several nuclei [36] a substantial reduction of the excitation strength of $D_{13}(1520)$ and $F_{15}(1680)$ resonances occur in comparison with the corresponding hydrogen and deuterium data. This effect suggests both a broadening of the resonance width and a quenching of their excitation strength [37]; while the broadening

could be a consequence of final state interactions [38], the quenching might be ascribed to a reduction of the transition strength in radial-type excitations, due again to the overlap of confinement potentials among neighbouring nucleons in nuclei [39]. However, a common explanation of the behaviour of the resonance bumps both in the photo- and in the electro-production still awaits for a deeper understanding.

5 Conclusions.

The concept of parton-hadron local duality represents a very powerful tool for analyzing inclusive lepton scattering data in the low Q^2 region, where important quantities like the mass scale, the leading and higher twists in the structure function may be investigated. We have analyzed all the existing inclusive data on the inelastic structure function of the nucleon, the deuteron and light complex nuclei in a Q^2 range from 0.3 to 5 $(GeV/c)^2$ and the Q^2 behaviours of the structure function and its moments have been presented for all the targets considered. In case of the proton we have observed that the Bloom-Gilman local duality is fulfilled only by the inelastic part of the structure function, while the inclusion of the contribution of the elastic peak leads to remarkable violations of the local duality. In case of complex nuclei, despite the poor statistics of the available data, our analysis suggests that the onset of the parton-hadron local duality for the inelastic part of the structure function is anticipated with respect to the case of the nucleon and the deuteron. A possible interpretation of this result in terms of a Q^2 -rescaling effect has been discussed: using different methods, a decrease of the mass scale of $\simeq 8\%$ in nuclei turns out to be consistent with inelastic experimental data. It has also been shown that the same variation of the mass scale is consistent with the faster fall-off of the $P_{33}(1232)$ transition form factors observed in nuclei with respect to the nucleon case even at very low values of Q^2 . Finally, we expect that the same Q^2 -rescaling effect cannot be applied both to the elastic and transition form factors of a nucleon bound in a nucleus, consistently with the severe constraints on nucleon swelling arising from updated analyses of the Coulomb sum rule in nuclei.

In conclusion, the Bloom-Gilman local duality in nucleon and nuclei appears to be a non-trivial dynamical property of the inelastic structure functions, whose deep understanding is still to be reached and deserves much more attention from the theoretical as well as the experimental point of view. As to the latter, more systematic and high-precision inclusive data are needed for a clear-cut extraction of information; our present analysis should therefore be considered as a strong suggestion that interesting results can be expected, when the structure functions of nucleon and nuclei are compared in the low Q^2 region. New facilities becoming operative in the next future, like *CEBAF*, are expected to provide inclusive data with unprecedented accuracy, allowing a throughout investigation of the relation among the physics in the nucleon-resonance and Deep Inelastic Scattering regions.

References

- [1] E. Bloom and F. Gilman: Phys. Rev. Lett. **25** (1970) 1140; Phys. Rev. **D4** (1971) 2901.

- [2] J.M. Laget in *New Vistas in Electro-Nuclear Physics*, edited by E.L. Tomusiak, H.S. Coplan and E.T. Dressler, NATO Advanced Study Institute, Series B, Vol. 142 (Plenum, New York, 1986), pp. 361-429, and references therein quoted.
- [3] M. Arneodo: *Phys. Rep.* **260** (1994) 302, and references therein quoted.
- [4] F. Heimlich et al.: *Nucl. Phys.* **A231** (1974) 509.
- [5] M. Anghinolfi et al.: *Nucl. Phys.* **A602** (1996) 405; *J. of Physics* **G21** (1995) L9.
- [6] A. De Rujula, H. Georgi and H.D. Politzer: *Ann. of Phys.* **103** (1977) 315.
- [7] H. Georgi and H.D. Politzer: *Phys. Rev.* **D14** (1976) 1829.
- [8] X. Ji and P. Unrau: *Phys. Rev.* **D52** (1995) 72.
- [9] M. Arneodo et al.: *Phys. Lett.* **B364** (1995) 107. L.W. Whitlow et al.: *Phys. Lett.* **B282** (1992) 475. M. Virchaux and A. Milsztajn: *Phys. Lett.* **B274** (1992) 221.
- [10] G. Altarelli and G. Parisi: *Nucl. Phys.* **B126** (1977) 298.
- [11] M. Gluck, E. Reya and A. Vogt: *Z. Phys.* **C53** (1992) 127; **C67** (1995) 433. H. Plochow-Besch: preprint /CERN-PPE/15-3-1995 (PDF Library) and *Comp. Phys. Comm.* **75** (1993) 396.
- [12] G. Altarelli, R.K. Ellis and G. Martinelli: *Nucl. Phys.* **B143** (1978) 521; *ib.* **B157** (1979) 461.
- [13] J.L. Miramontes, M.A. Miramontes and J. Sanchez Guillen: *Phys. Rev.* **D40** (1989) 2184; *Z. Phys.* **C41** (1988) 247.
- [14] K. Bitar, P.W. Johnson and Wu-Ki Tung: *Phys. Lett.* **B83** (1979) 114. R.K. Ellis, L. Petronzio and G. Parisi: *Phys. Lett.* **B64** (1976) 97.
- [15] A. Bodek et al.: *Phys. Rev.* **D20** (1979) 7. S. Stein et al.: *Phys. Rev.* **D12** (1975) 1884.
- [16] S. Simula: *Few Body Systems Suppl.* **8** (1995) 423; *ibidem* **9** (1995) 466.
- [17] L.L. Frankfurt and M.I. Strikman: *Phys. Rep.* **76** (1981) 215.
- [18] M. Lacombe et al.: *Phys. Lett.* **B101** (1981) 139.
- [19] M. Arneodo et al.: *Nucl. Phys.* **B33** (1990) 1.
- [20] D.T. Baran et al.: *Phys. Rev. Lett.* **61** (1988) 400.
- [21] E. Rondio, private communication.
- [22] J. Gomez et al.: *Phys. Rev.* **D49** (1994) 4348.

- [23] J. Franz et al.: Z. Phys. **C10** (1981) 105.
- [24] (a) D.B. Day et al.: Phys. Rev. **C48** (1993) 1849. (b) F. Heimlich et al.: Phys. Rev. **C3** (1971) 1448. (c) R.M. Sealock et al.: Phys. Rev. Lett. **62** (1989) 1350.
- [25] C. Ciofi and S. Simula: Phys. Rev. **C53** (1996) 1689; Phys. Lett. **B325** (1994) 276.
- [26] R. Cenni and P. Saracco: J. of Phys. **G20** (1994) 727.
- [27] R. Jaffe: Phys. Rev. Lett. **50** (1983) 228. F.E. Close, R.G. Roberts and G.G. Ross: Phys. Lett. **B129** (1983) 346. F. Close, R. Jaffe, A. Roberts and G. Ross: Phys. Lett. **bf B134** (1984) 449; Phys. Rev. **D31** (1985) 1004.
- [28] G.V. Dunne and A. W. Thomas: Nucl. Phys. **A455** (1986) 701.
- [29] W. Zhu and L. Qian: Phys. Rev. **C45** (1992) 1397.
- [30] A.C. Benvenuti et al.: Phys. Lett. **B195** (1987) 91.
- [31] C.E. Carlson and N.C. Mukhopadhyay: Phys. Rev. **D47** (1993) R1737.
- [32] I. Sick: Phys. Lett. **B157** (1985) 13.
- [33] J.P. Chen et al.: Phys. Rev. Lett. **66** (1991) 1283.
- [34] J. Jourdan: Nucl. Phys. **A603** (1996) 117.
- [35] M. Anghinolfi et al.: Phys. Rev. **C47** (1993) R922. Th. Frommhold et al.: Phys. Lett. **B295** (1992) 28. G. Ricco: in Proc. of the 4th Int. Seminar on Nuclear Physics, Amalfi (Italy), May 1992, ed. A. Covello (World Scientific, Singapore, 1993), p.57.
- [36] M. Bianchi et al.: Phys. Lett. **B299** (1993) 219; *ib.* **B325** (1994) 333.
- [37] V. Mokeev, E. Santopinto, M. Giannini and G. Ricco: Int. J. Mod. Phys. **E4** (1995) 607.
- [38] W.M. Alberico, G. Gervino and A. Lavagno: Phys. Lett. **B231** (1994) 177. L. Kondratyuk, M. Krivoruchenko, N. Bianchi, E. De Sanctis and V. Muccifora: Nucl. Phys. **A579** (1994) 453.
- [39] M. Giannini and E. Santopinto: Phys. Rev. **C49** (1994) R1258. M. Giannini and E. Trovatore: Int. J. Mod. Phys. **E**, in press.

Table 1. Values of $Q^2 = Q_0^2$ (in GeV^2/c^2) where a systematic change in the slope is exhibited by the Q^2 -dependence of the moments $M_2(Q^2)$, $M_4(Q^2)$ and $M_6(Q^2)$ (see Fig. 5), computed for the proton, the deuteron and nuclei with $A \simeq 12$ according to Eq. (1) using the experimental data shown in Figs. 1, 2 and 4.

	M_2	M_4	M_6
<i>proton</i>	1.6 ± 0.2	1.5 ± 0.1	1.6 ± 0.1
<i>deuteron</i>	1.6 ± 0.1	1.5 ± 0.1	1.5 ± 0.1
<i>nuclei</i>	0.8 ± 0.1	1.0 ± 0.2	1.2 ± 0.1

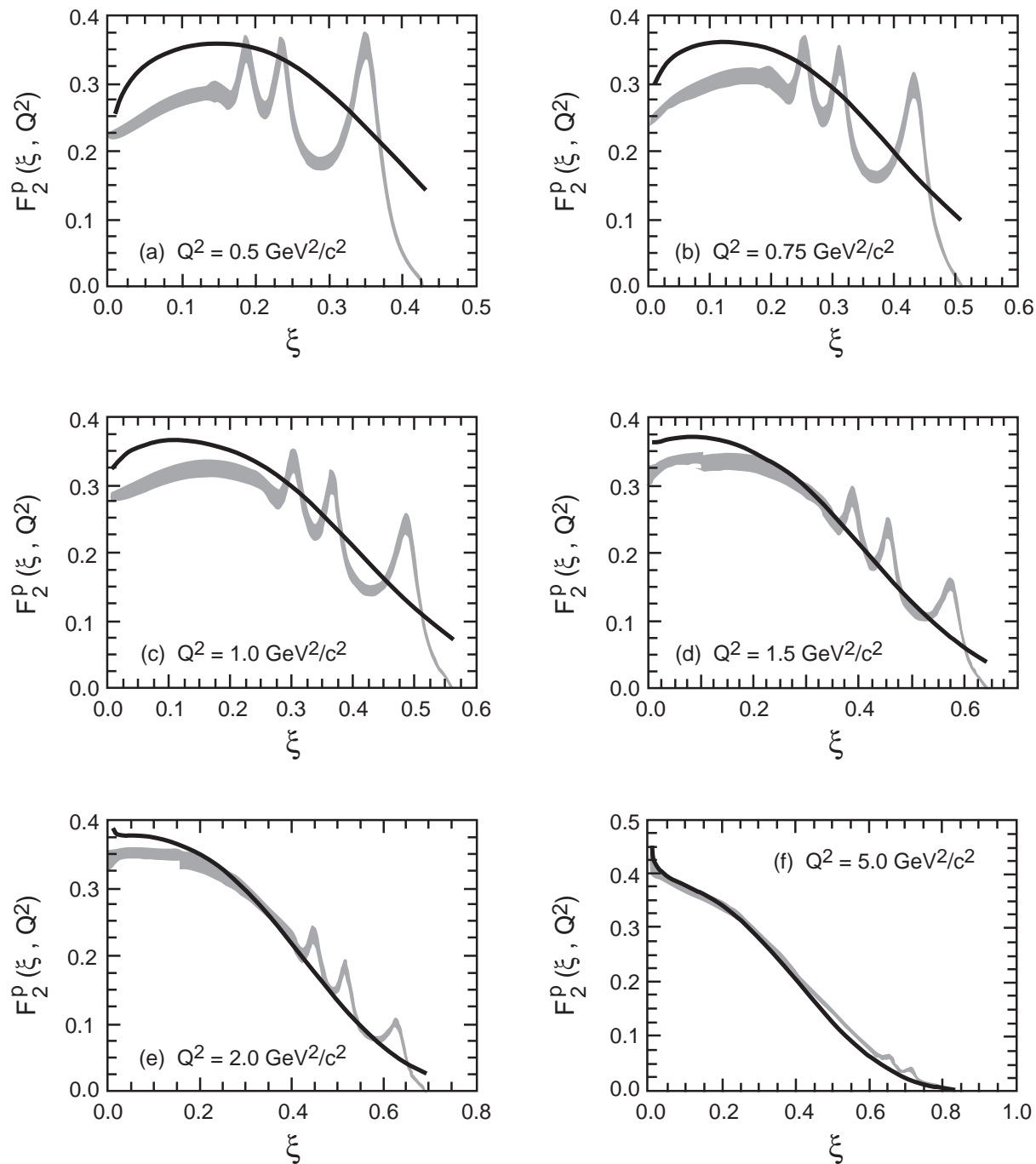


Figure 1. Proton structure function $F_2^p(\xi, Q^2) = \nu W_2^p(\xi, Q^2)$ versus the Nachtmann variable ξ (Eq. (2)) at various values of Q^2 . The shaded areas represent the pseudo-data, obtained from a fit of *SLAC* data at medium and large x [15] and from a fit of *NMC* data [9] in the *DIS* region, including the total uncertainty of the fits. The solid lines are the *dual* structure function of the nucleon (Eq. (4)), obtained starting from the *GRV* [11] parton densities evolved *NLO* at low Q^2 and target-mass corrected according to Ref. [7].

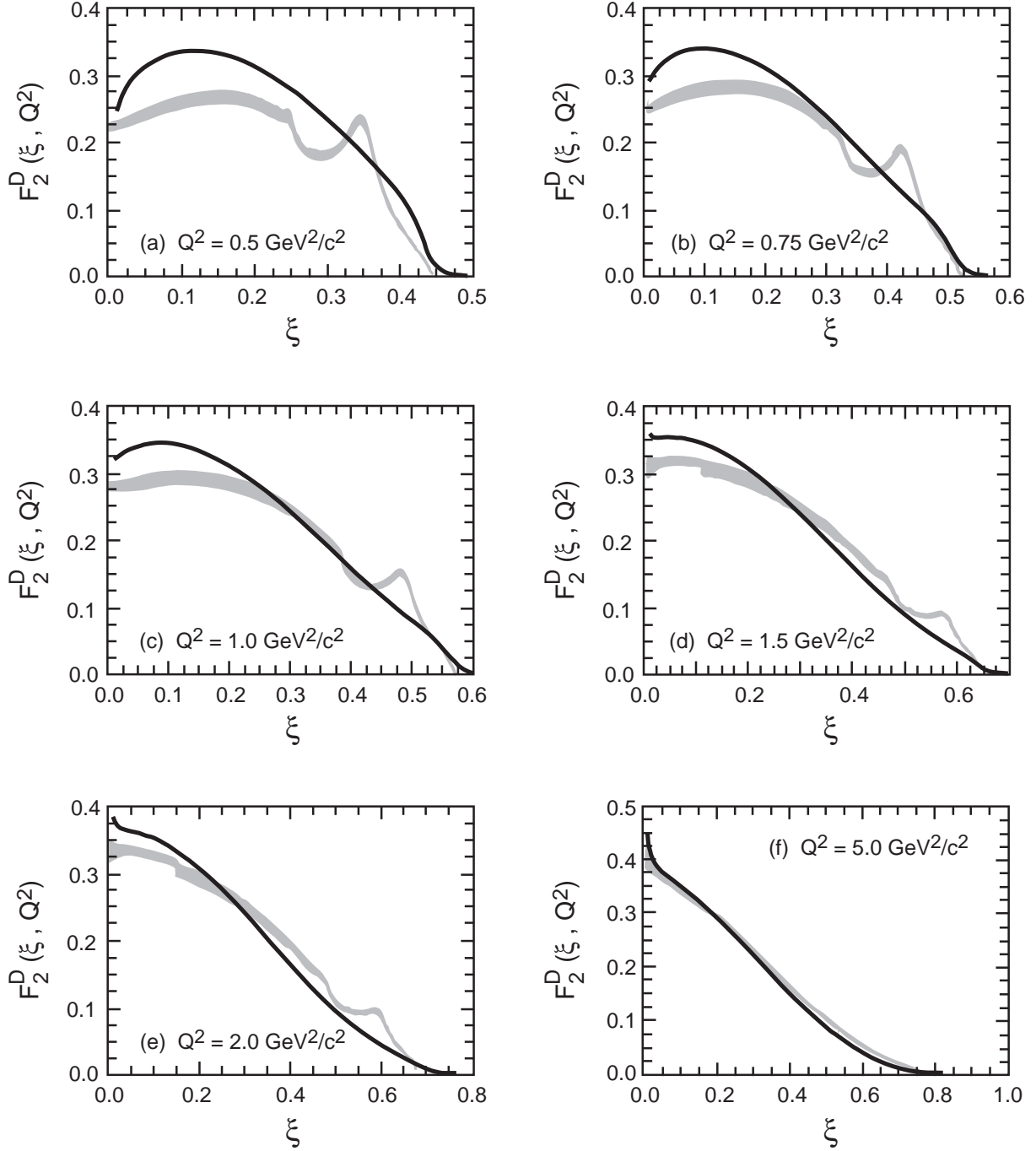


Figure 2. The same as in Fig. 1, but for the deuteron structure function per nucleon $F_2^D(\xi, Q^2) \equiv \nu W_2^D(\xi, Q^2)/2$. The *NMC* data of Ref. [19] at low ξ and the fits of inclusive data given in Refs. [9] and [15], have been considered. The solid curve is the *dual* structure function of the nucleon (Eq. (4)), folded according to the procedure of Ref. [16] with the nucleon momentum distribution in the deuteron corresponding to the Paris nucleon-nucleon potential [18].

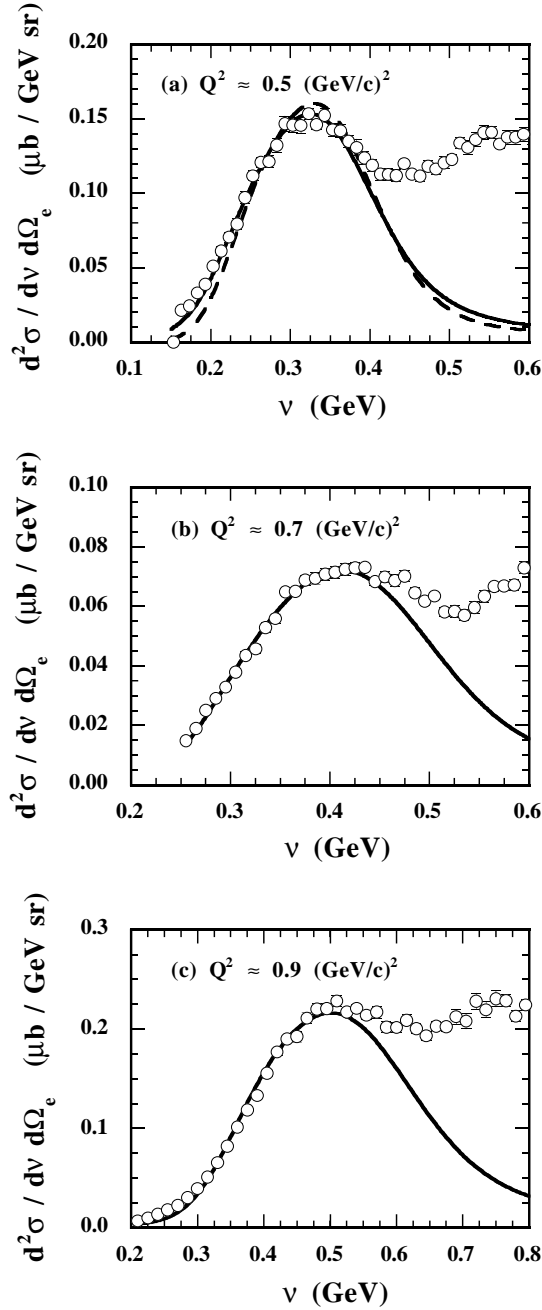


Figure 3. Differential cross section (per nucleon) for the inclusive process $^{12}\text{C}(e, e')X$ versus the energy transfer ν in the Q^2 range from 0.5 to 0.9 $(\text{GeV}/c)^2$ (at the quasi-elastic peak). The solid lines represent the quasi-elastic contribution calculated using the approach of Ref. [25], which includes final state interaction effects. In (a) the dashed line is the same as the solid line, but obtained within the impulse approximation only, i.e. without including final state interaction effects. In (a), (b) and (c) the electron beam energy and scattering angle, (E_e, θ_e) , are: $(1.3 \text{ GeV}, 37.5^\circ)$, $(1.5 \text{ GeV}, 37.5^\circ)$ and $(3.595 \text{ GeV}, 16^\circ)$, respectively. In (a) and (b) the experimental data are from Ref. [24](c), while in (c) they are from Ref. [24](a).

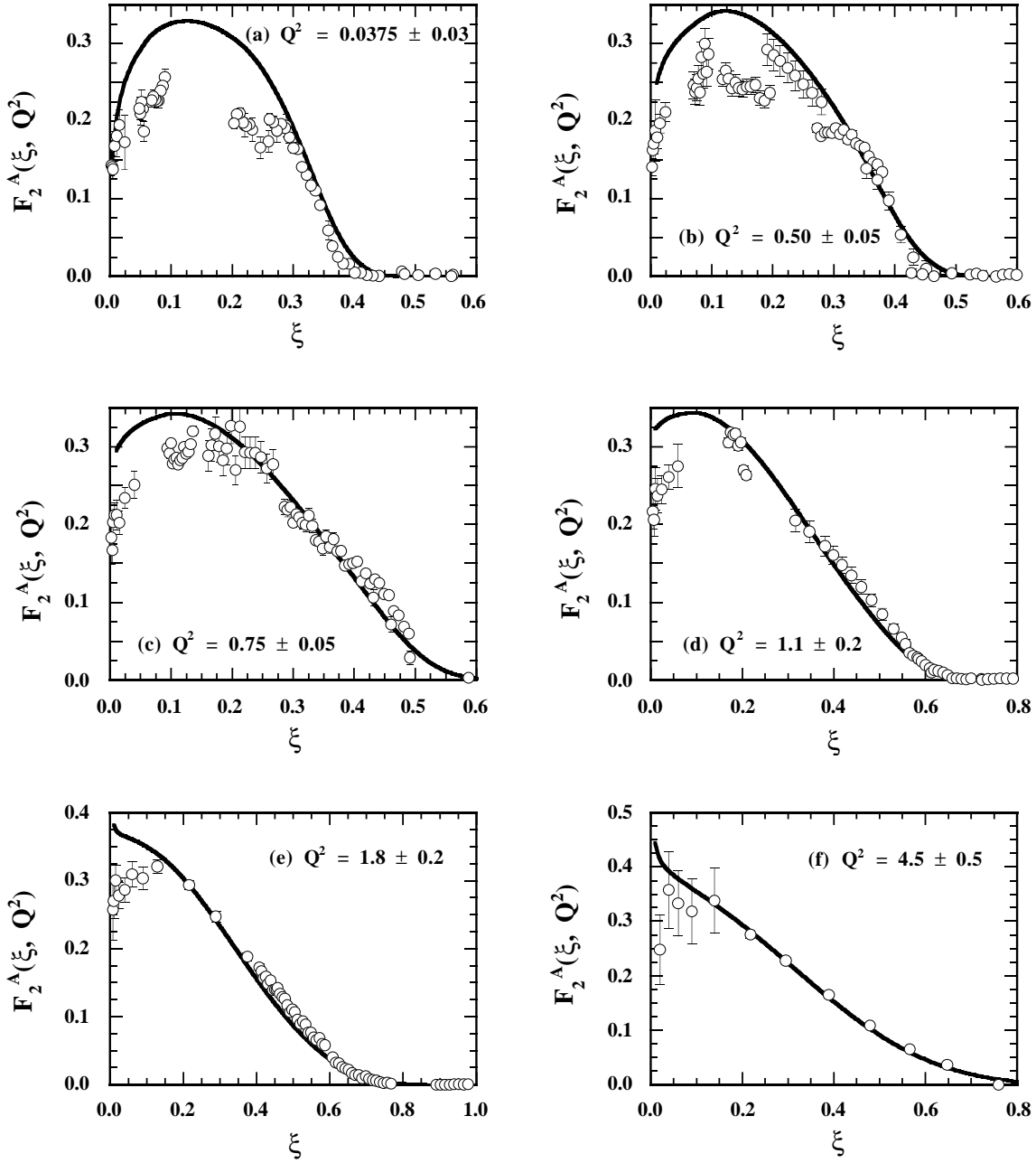


Figure 4. The same as in Fig. 1, but for the nuclear structure function per nucleon $F_2^A(\xi, Q^2) \equiv \nu W_2^A(\xi, Q^2)/A$ in case of nuclei with $A \simeq 12$. Experimental data are from Refs. [22, 23] (${}^9\text{Be}$), [15, 19, 24] (${}^{12}\text{C}$) and [5] (${}^{16}\text{O}$). The solid curve is the *dual* structure function of the nucleon (Eq. (4)), folded according to the procedure of Ref. [16], which adopts the nucleon spectral function of Ref. [25] to take into account nuclear binding effects.

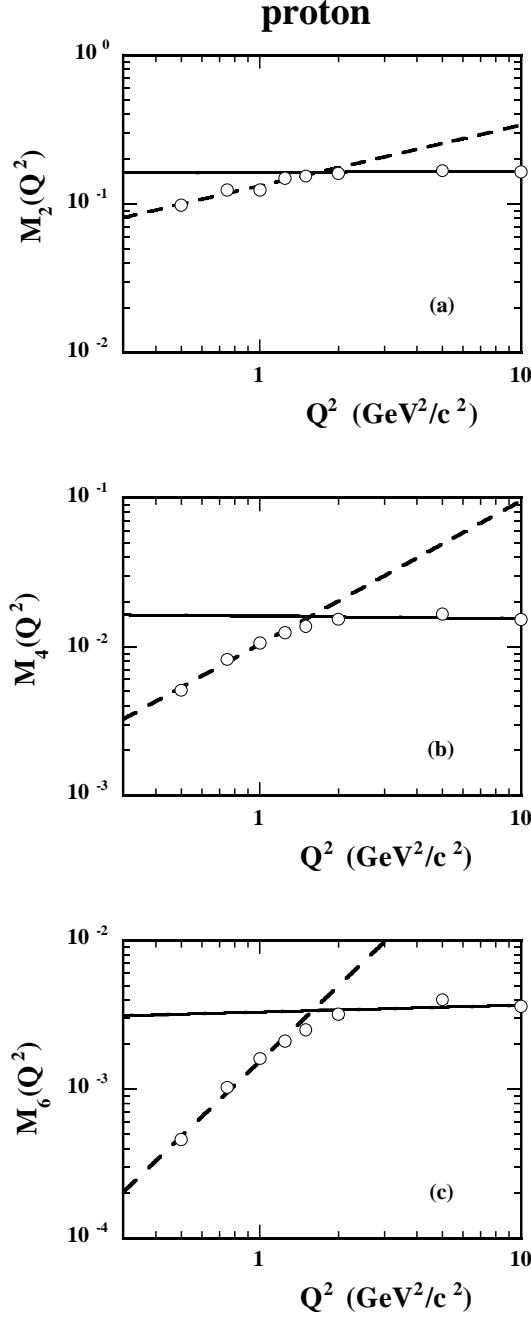


Figure 5. The moments $M_2(Q^2)$, $M_4(Q^2)$ and $M_6(Q^2)$, computed according to Eq. (1) for the proton (a,b,c), the deuteron (d,e,f) and nuclei with $A \simeq 12$ (g,h,i) using the experimental data of Figs. 1, 2 and 4, versus Q^2 . The dashed and solid lines are linear fits to low and high Q^2 points and they are intended to show up the change of the slope of the moments at $Q^2 \simeq Q_0^2$.

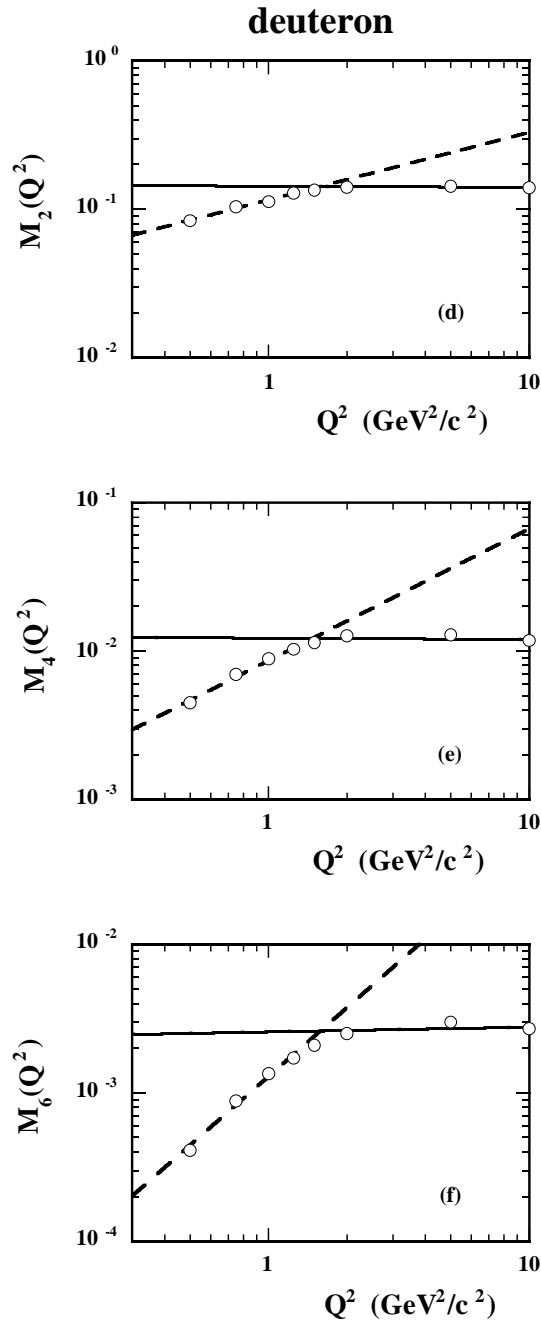


Figure 5 - continued.

nuclei

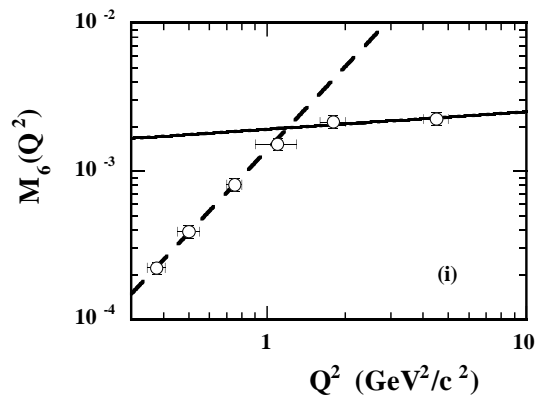
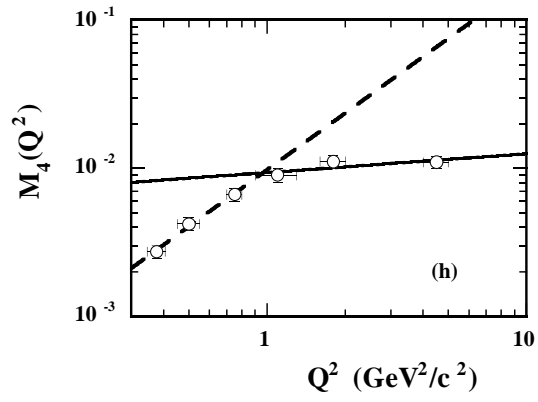
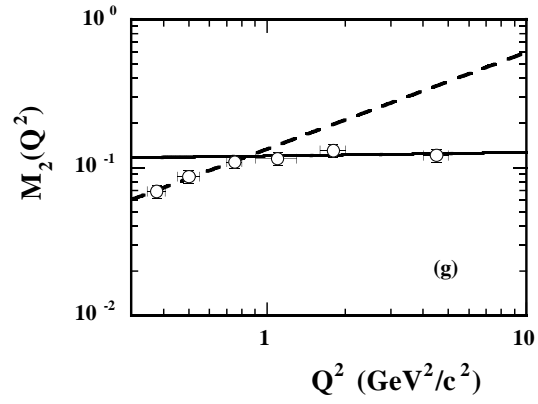


Figure 5 - continued.

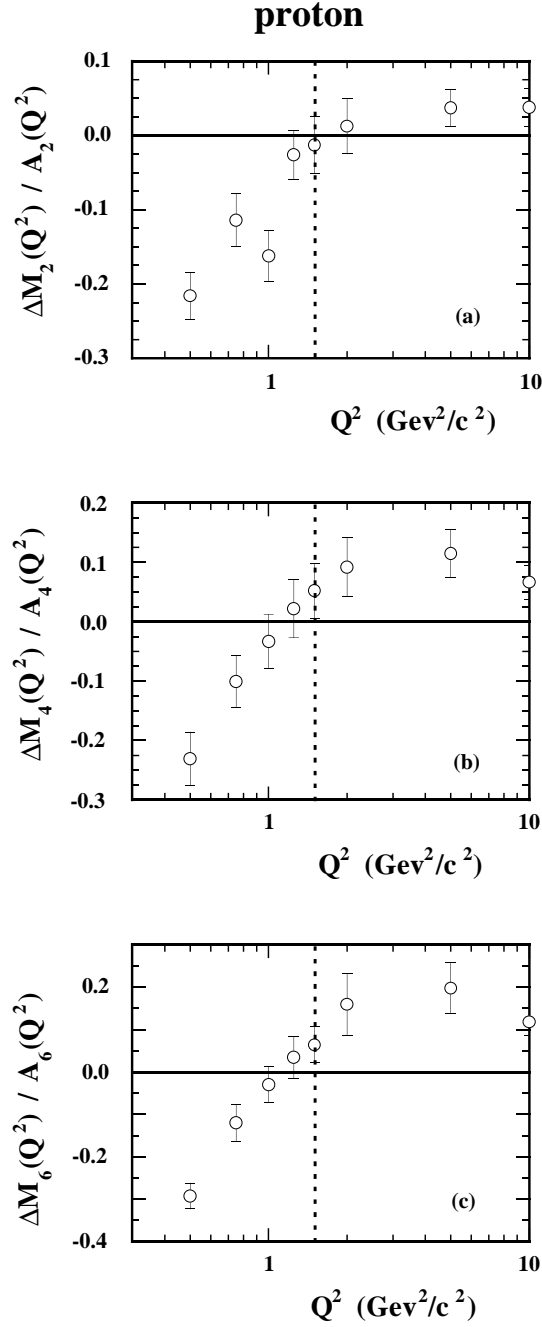


Figure 6. The relative deviation $\Delta M_n(Q^2)/A_n(Q^2)$ (Eq. (6)) of the *experimental* moments $M_n(Q^2)$, reported in Fig. 5, with respect to the leading twist moments $A_n(Q^2)$, calculated from Eq. (1) using the *dual* nucleon structure function (4), properly folded [16] with the nucleon motion in the nuclear medium. The vertical dotted lines are intended to show the approximate location of the static point $Q^2 \simeq \mu^2$, namely $\mu_N^2 \simeq \mu_D^2 \simeq 1.5$ (GeV/c)² and $\mu_A^2 \simeq 1.0$ (GeV/c)² (see text).

deuteron

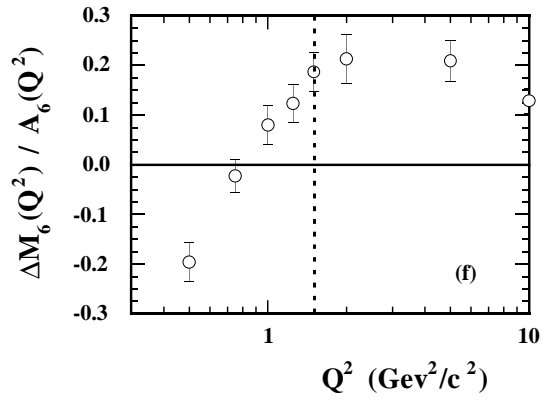
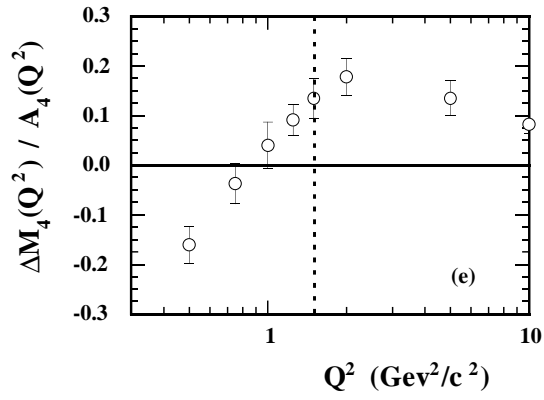
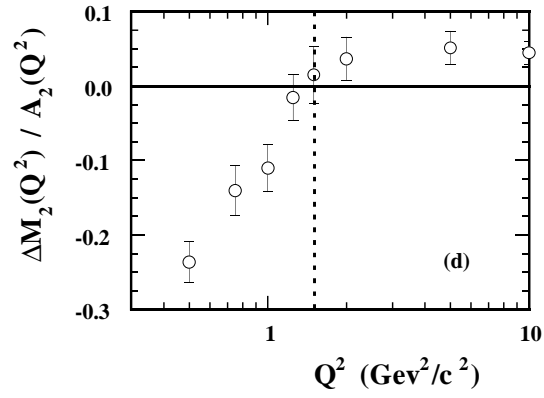


Figure 6 - continued.

nuclei

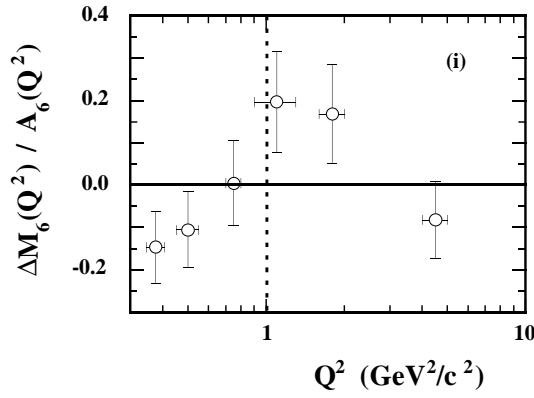
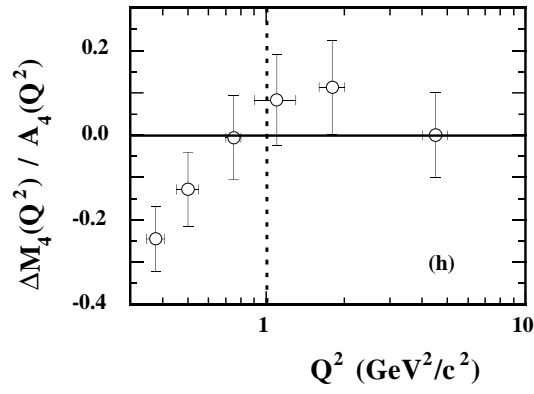
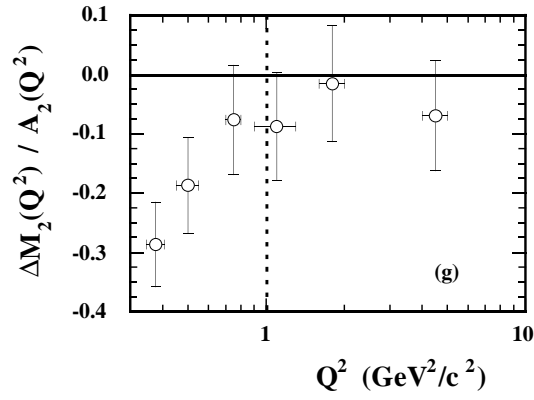


Figure 6 - continued.

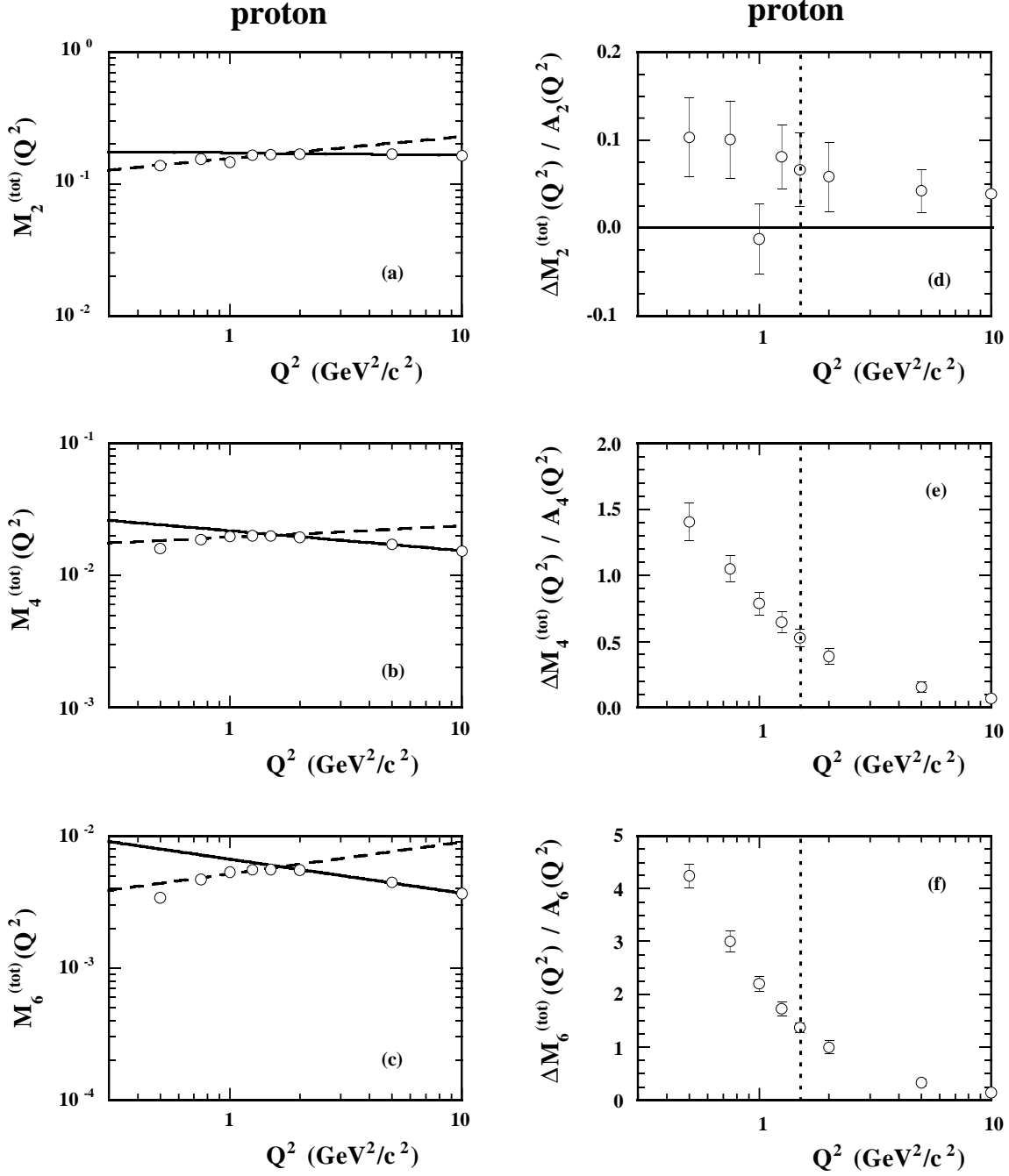


Figure 7. The moments $M_n^{(tot)}(Q^2) = M_n^{(el)}(Q^2) + M_n(Q^2)$ (a, b, c) and the relative deviation $\Delta M_n^{(tot)}(Q^2)/A_n(Q^2)$ (d, e, f), calculated for the proton including in Eq. (1) the contribution of the elastic peak (7), versus Q^2 . The vertical dotted lines are the same as in Fig. 6 (a, b, c).

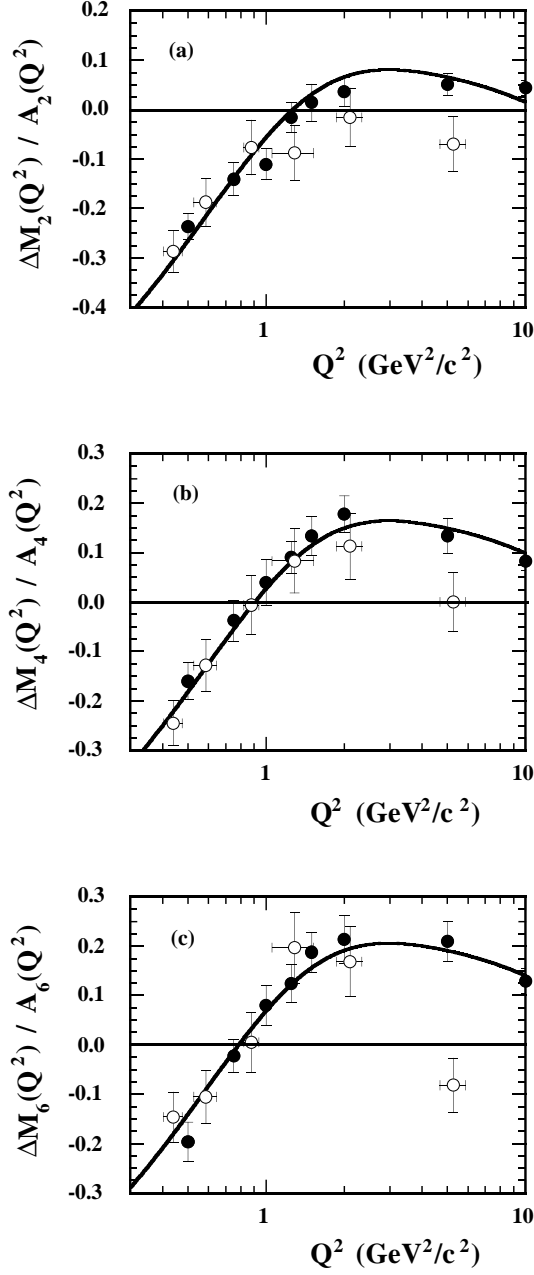


Figure 8. The relative deviation $\Delta M_n(Q^2)/A_n(Q^2)$ (Eq. (6)) of the *experimental* moments $M_n(Q^2)$ calculated for the deuteron (black dots) and for nuclei with $A \simeq 12$ (open dots). The latter have been Q^2 -rescaled according to Eq. (8) using $\delta_n(Q^2 \simeq \mu^2) \simeq \mu_D^2/\mu_A^2 = 1.17$. The solid lines represent global fits of the deuteron and (Q^2 -rescaled) nuclear points.

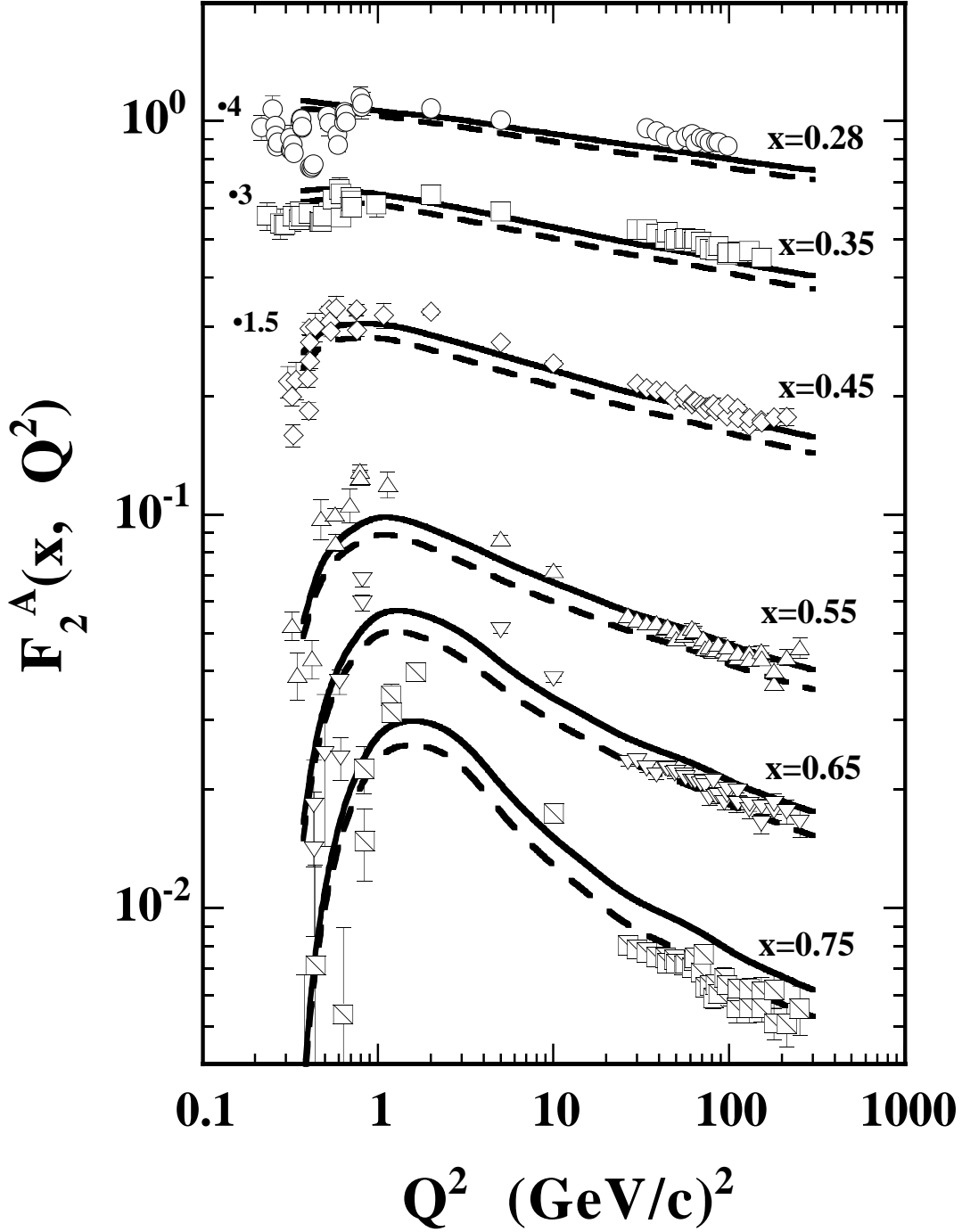


Figure 9. Nuclear structure function per nucleon $F_2^A(x, Q^2) \equiv \nu W_2^A(x, Q^2)/A$ versus Q^2 at fixed values of x in case of nuclei with $A \simeq 12$. The experimental data are from Refs. [5, 15, 19, 22, 23, 24, 30]. The various markers correspond to different values of x . The solid line is the folding of the *dual* nucleon structure function (Eq. (4)) obtained using the procedure of Ref. [16]. The dashed line is the same as the solid line, but using the rescaling relation (9) with $\delta(Q^2)$ taken from Ref. [27] and $\mu_D/\mu_A = 1.10$.

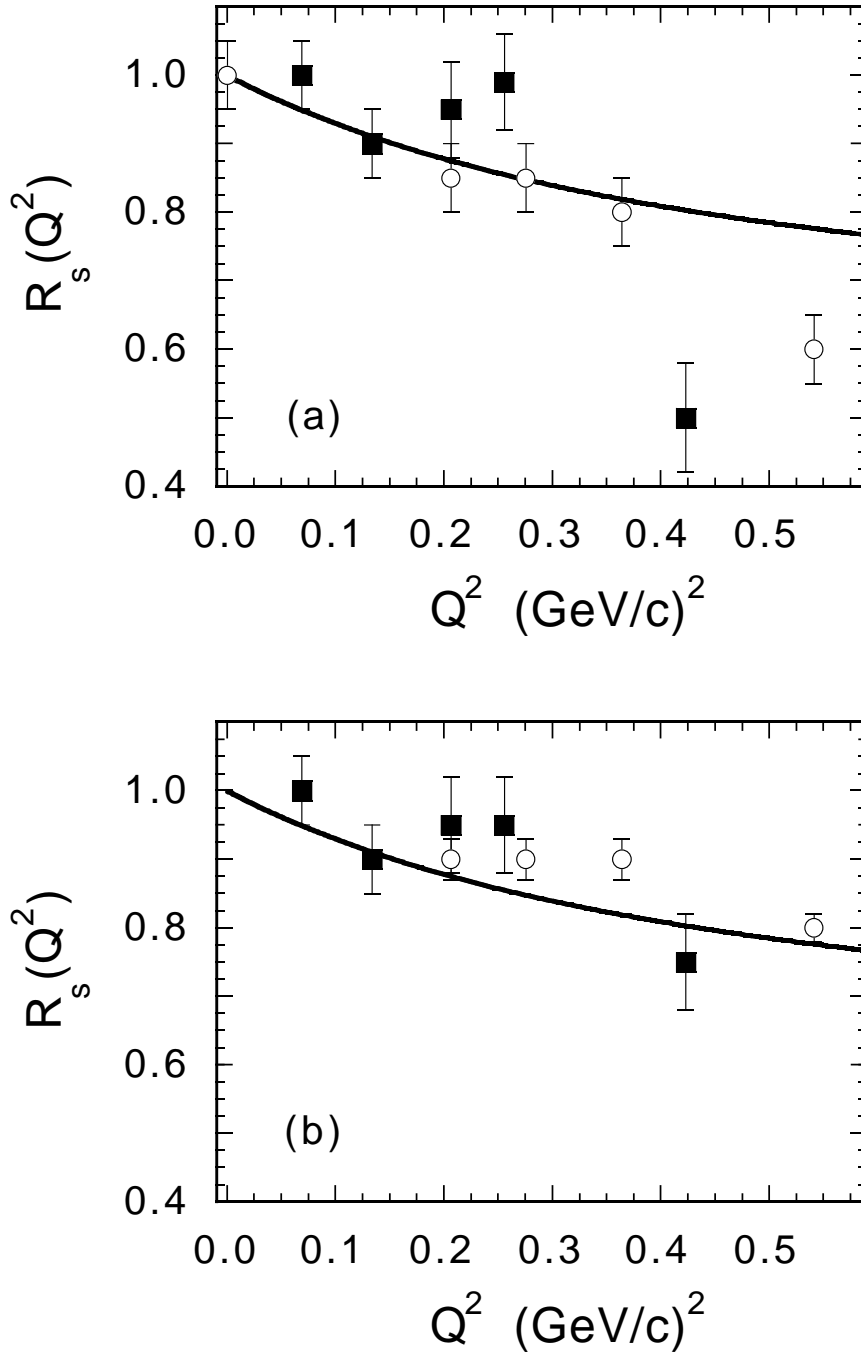


Figure 10. The suppression factor $R_s(Q^2)$ versus Q^2 , as determined in Ref. [5], using inclusive ^{12}C (open dots) and ^{16}O data (full squares), in case of the excitation of the $P_{33}(1232)$ resonance only (a) and for the total inclusive cross section @ $W = 1232 \text{ MeV}$ (b). The solid line is the prediction of the rescaling relation (10), obtained adopting a dipole ansatz for the magnetic form factor of the $N - \Delta$ transition, $G_M^{(N-\Delta)}(Q^2)$, and the value $\mu_D/\mu_A = 1.08$.